

## RED-ACT Report

### Real-time Earthquake Damage Assessment using City-scale Time-history analysis

#### May. 5, M5.3 Japan Nemuro-hanto Nanto-oki Earthquake

Research group of Xinzheng Lu at Tsinghua University (luxz@tsinghua.edu.cn)

First reported at 06:00, May. 5, 2019 (Beijing Time, UTC +8)

#### Acknowledgments and Disclaimer

The authors are grateful for the data provided by **K-NET** and **KiK-net**. This analysis is for research only. The actual damage resulting from the earthquake should be determined according to the site investigation.

#### Scientific background of this report can be found at:

[http://www.luxinzheng.net/software/Real-Time\\_Report.pdf](http://www.luxinzheng.net/software/Real-Time_Report.pdf)

### 1. Introduction to the earthquake event

At 01:40 05 May 2019 (Local Time, UTC +9), an **M 5.3 (JMA)** earthquake occurred in **Japan Nemuro-hanto Nanto-oki**. The epicenter was located at **146.4 43.2**, with a depth of **60.0 km**.

### 2. Recorded ground motions

**10** ground motions near to epicenter of this earthquake were analyzed. The names and locations of the stations can be found Table 1. The maximal recorded peak ground acceleration (PGA) is **164 cm/s/s**. The corresponding response spectra in comparison with the design spectra specified in the Chinese Code for Seismic Design of Buildings are shown in Figure 1.

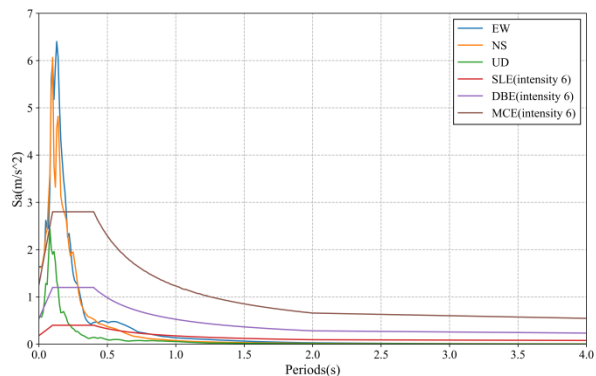


Figure 1 Response spectra of the recorded ground motions with maximal PGA

### 3. Damage analysis of the target region subjected to the recorded ground motions

Using the real-time ground motions obtained from the strong motion networks and the **city-scale nonlinear time-history analysis (see the Appendix of this report)**, the damage ratios of buildings located in different places can be obtained. The building damage distribution and the human uncomfotableness distribution near to different stations is shown in Figure 2 and Figure 3, respectively. These outcomes can provide a reference for post-earthquake rescue work.

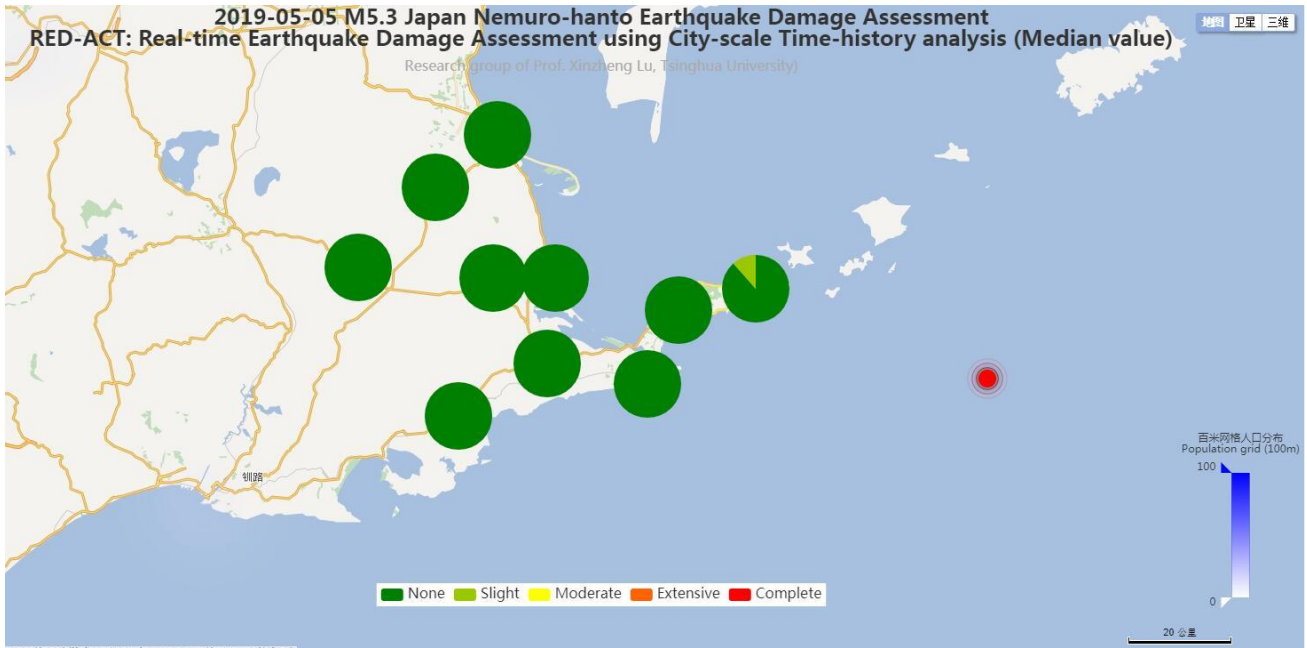


Figure 2 Damage ratio distribution of the buildings near to different stations

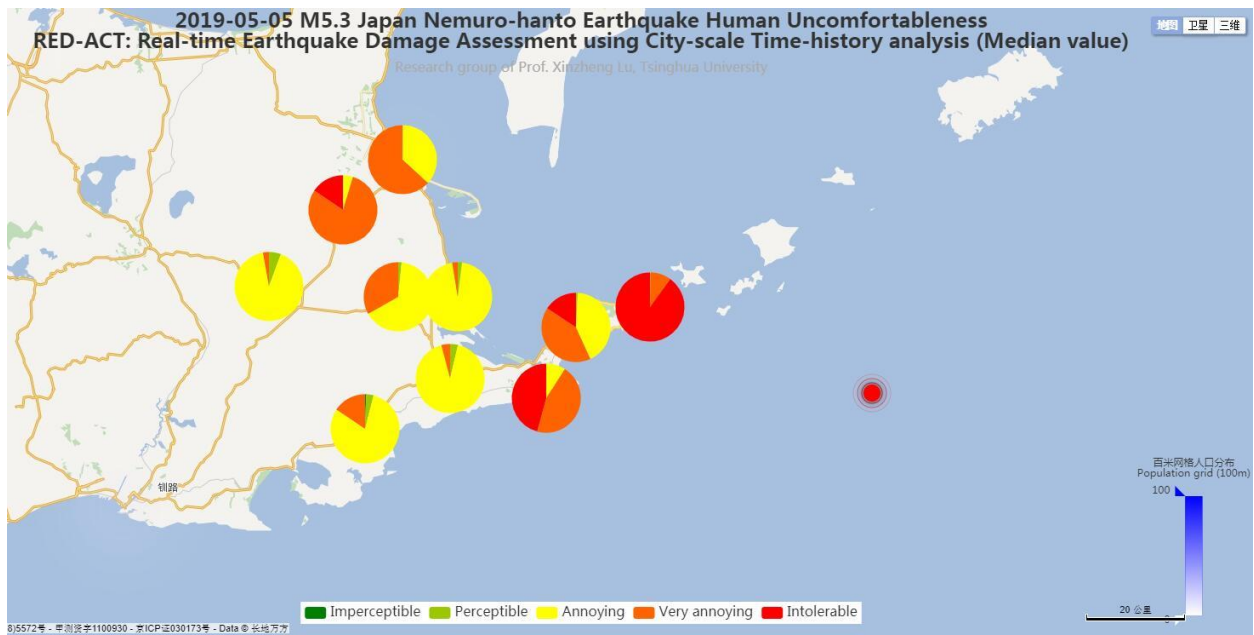
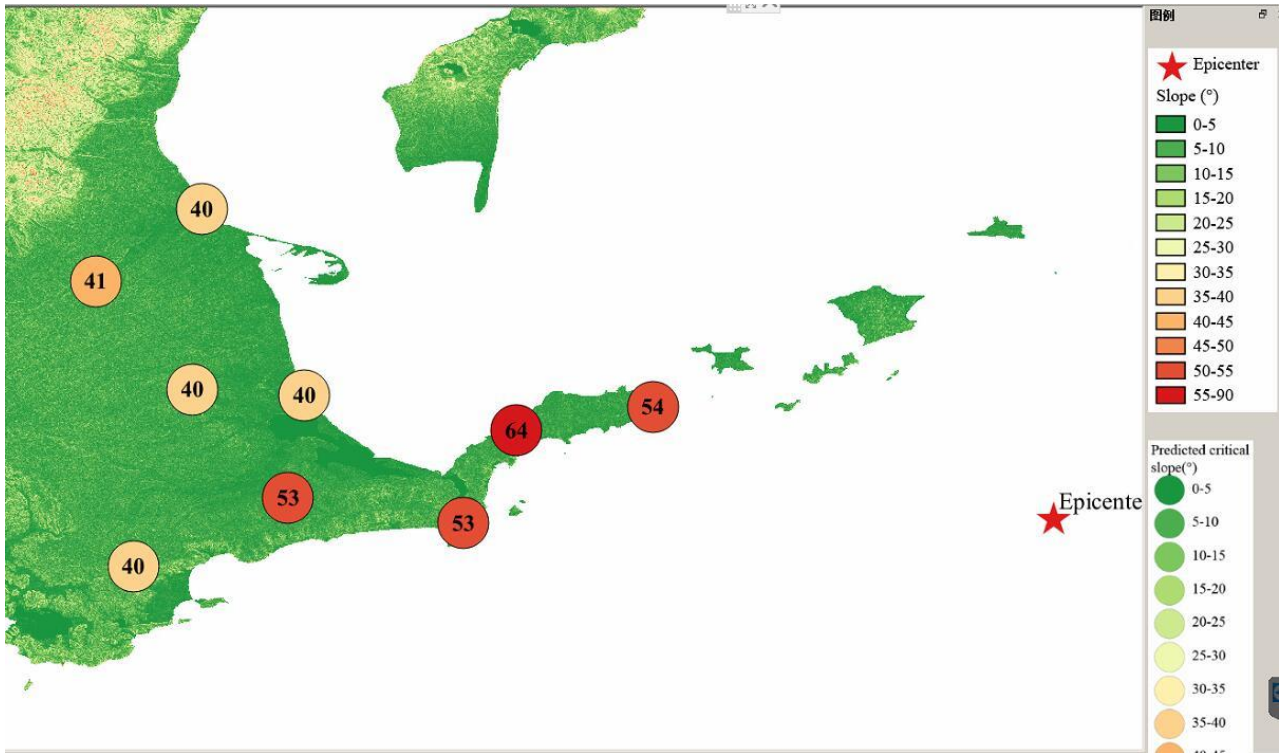


Figure 3 Human uncomfortableness distribution near to different stations

#### 4. Earthquake-induced landslide of the target region subjected to the recorded ground motions

According to local topographic data, lithology data and ground motion records, the distribution of earthquake-induced landslide near to different stations under the different proportions of the landslide slab thickness that is saturated can be calculated, as shown in Figure 4. The basemap shows the distribution of the local slope. The number in the circle represents the critical slope of the landslide. The earthquake-induced landslide tends to occur with a higher probability when the slope is larger than this threshold value.



(a) The proportion of the landslide slab thickness that is saturated equals 0%



(b) The proportion of the landslide slab thickness that is saturated equals 50%



(c) The proportion of the landslide slab thickness that is saturated equals 90%  
 Figure 4 Distribution of earthquake-induced landslide near to different stations

Scientific background of this report can be found at: [http://www.luxinzheng.net/software/Real-Time\\_Report.pdf](http://www.luxinzheng.net/software/Real-Time_Report.pdf)

Table 1 Names and locations of the strong motion stations

No.	Station Name	Longitude	Latitude
1	HKD066	145.131	43.6619
2	HKD067	144.973	43.555
3	HKD068	144.77	43.4108
4	HKD069	145.117	43.3941
5	HKD070	145.284	43.3852
6	HKD071	145.26	43.2326
7	HKD072	145.521	43.1948
8	HKD073	145.6	43.3327
9	HKD074	145.803	43.368
10	HKD075	145.029	43.1309

